American Mineralogist, Volume 78, pages 1016–1030, 1993

Pressure effects, kinetics, and rheology of anorthositic and related magmas

JOHN LONGHI
Lamont-Doherty Geological Observatory of Columbia University, Palisades, New York 10964, U.S.A.
MIRANDA S. FRAM
Department of Geological Sciences and Lamont-Doherty Geological Observatory of Columbia University, Palisades, New York 10964, U.S.A.
JACQUELINE VANDER AUWERA
Laboratoires associés de Géologie, Pétrologie, Géochimie-B20-Université de Liège, B-4000 Sart Tilman, Belgium
JENNIFER N. MONTIETH
Department of Geological Sciences and Lamont-Doherty Geological Observatory of Columbia University, Palisades, New York 10964, U.S.A.

ABSTRACT

Anhydrous experiments on natural and synthetic starting materials with basaltic to anorthositic bulk compositions show a systematic increase in the albite component of near-liquidus plagioclase and in the Al_2O_3 content of orthopyroxene with increasing pressure. These results are consistent with crystallization of the highly aluminous orthopyroxene megacrysts and most of the plagioclase in massif anorthosite complexes at lower crustal pressures. Comparison of plagioclase compositions from near-liquidus and subliquidus experiments conducted in this laboratory with plagioclase compositions predicted at 1 atm for the experimental temperature and liquid compositions by various empirical models indicates that the shift to more albitic plagioclase is predominantly a pressure effect on the partitioning of albite (Ab) and anorthite (An) components between plagioclase and liquid. However, even when pressure terms are added to the models for Ab and An partitioning, there remain statistically significant compositional dependencies that are most apparent when the liquid composition is nepheline normative. These compositional dependencies probably arise from the absence of highly aluminous and nepheline-normative liquids in the data from which the models were constructed. Accordingly, we present empirical adjustments to the plagioclase-liquid models of Drake (1976), Weaver and Langmuir (1990), and Ariskin and Barmina (1990).

The positive pressure dependence of Al_2O_3 in orthopyroxene coexisting with plagioclase and liquid is almost entirely the result of changes in orthopyroxene-liquid partitioning and not related to increases in the Al_2O_3 concentration of the liquid. Data for Al_2O_3 partitioning from 46 orthopyroxene-liquid and 45 pigeonite-liquid pairs taken from the literature show that pressure is the most important control on the simple molar partition coefficient for Al_2O_3. Rapid crystal growth is rejected as an alternative explanation for the high Al_2O_3 contents of orthopyroxene megacrysts because rapid growth leads to low Cr_2O_3 concentrations in orthopyroxene, contrary to what is observed.

These results support polybaric models for massif anorthosite petrogenesis that entail accumulation of plagioclase in evolved basaltic magma chambers ponded in the lower crust followed by buoyant ascent of plagioclase-rich magmatic suspensions that intrude the upper crust, carrying rafts of orthopyroxene megacrysts. In thick, decompressing suspensions, the interplay of tie-line rotation and mass balance prevents plagioclase from becoming significantly more anorthitic. Experimental studies suggest that the transition from liquid- to solid-state rheology of plagioclase suspensions occurs at ~60% crystallinity for a homogeneous grain-size distribution and near static conditions. However, both motion of the suspension and uneven grain-size distribution shift the transition to higher crystallinities. Thus the transit of suspensions with leuconoritic composition (65–70% plagioclase) may be possible with minimal deformation of the entrained plagioclase. Formation of deformed anorthosite masses may then occur as second-stage buoyant segregations within the upper crustal magma chambers.

0003–004X/93/0910–1016$02.00

Introduction

Proterozoic massif anorthosite complexes have two important features that have been ascribed to crystallization of broadly basaltic magmas at lower crustal and upper mantle pressures: a predominance of plagioclase with intermediate composition (An_{35}–An_{65}) and the presence of scattered megacrysts of highly aluminous orthopyroxene. In the former case, experimental evidence from anhydrous systems that liquidus plagioclase becomes more albitic with increasing pressure was cited as evidence that massif anorthosites were emplaced in the lower crust (Green, 1969). Experimental data indicating that the Al_2O_3 concentration in orthopyroxene coexisting with plagioclase increases with increasing pressure have been cited as evidence that the megacrysts also crystallized at lower crustal pressures (Emslie, 1975; Maquil, 1978). However, more recent geobarometric studies of contact aureoles have shown that massif anorthosites were emplaced in the middle to upper crust (Berg, 1977; Valley and O'Neill, 1978; Fuhrman et al., 1988). This apparent difference between pressures of crystallization and emplacement is the basis for a series of polybaric petrogenetic models for massif anorthosites that involve accumulation of plagioclase from a basaltic parent magma ponded in the lower crust, followed by the intrusion of a plagioclase-rich suspension or mush into the middle to upper crust (e.g., Duchesne, 1984; Longhi and Ashwal, 1984; Emslie, 1985). Although both the change in liquidus plagioclase composition and the increase in Al_2O_3 concentration in orthopyroxene with pressure are supported by experimental data (Green, 1969; Maquil, 1978), some of the data are suspect because of short experiment times and the lack of clear reversal of mineral compositions. In this paper we examine experimental data from the literature and some new data from this laboratory that confirm the shift to more albitic plagioclase and more aluminous orthopyroxene with increasing pressure in anhydrous systems. We use the data to modify existing models of Ab-An partitioning between plagioclase and liquid, to construct new models for Al_2O_3 partitioning between orthopyroxene and liquid, and to examine kinetic models for producing aluminous orthopyroxene. Finally, we examine some of the mass-balance and rheological aspects of plagioclase-rich magmas.

Experimental methods

All of the experiments from our laboratory were carried out under nearly volatile-free conditions in graphite capsules in ½-in. solid media piston-cylinder apparati according to the methods described by Fram and Longhi (1992). Typical experiment durations were 1–4 d. Starting materials consisted of two powdered rocks and one synthetic glass. One rock, 500B, is from an anorthositic dike in the Nain Province of Labrador, described by Wiebe (1979, 1990); all the 500B data are taken from Fram and Longhi (1992). The other rock, TJ, is a monzonorite taken from the chill margin of the Bjerkreim-Sokndal layered intrusion near Tjørn in the Rogaland province of Norway (Duchesne and Hertogen, 1988). TJ has plagioclase alone on the liquidus to at least 13 kbar (Vander Auwera and Longhi, 1992); complete details of the experiments and phase compositions will be presented elsewhere. The synthetic glass, HLCA, has the composition of the average high-Al gabbro in the Harp Lake Complex of Labrador and is proposed to represent the parent liquid composition of the Harp Lake anorthosites (Emslie, 1980). All of the isobaric experimental data on HLCA are taken from Fram and Longhi (1992). As part of this study, some of the orthopyroxene compositions produced in the isobaric experiments on HLCA were reversed in polybaric experiments. These experiments had two stages. The first stage was a conventional isobaric experiment (1–2 d) with HLCA starting material loaded into graphite capsules bored out to increase the size of the charge. At the end of the experiment the charge was recovered, ground in an agate mortar, mixed with sufficient amounts of the original glass starting material to fill a standard-sized capsule, and then held at a new temperature and pressure for approximately 5 d. Following the second stage, the charges were mounted in epoxy, polished, and analyzed with a Cameca Camebax electron microprobe according to the procedures described by Fram and Longhi (1992).

Results

Plagioclase/liquid

Figure 1 illustrates the compositions of plagioclase along the liquidi of 500B, HLCA, and TJ as a function of pressure. Also shown are the compositions of plagioclase in the 500B and TJ starting materials. There are two important features. First, the range of plagioclase compositions is dramatically narrower in the experiments than in 500B—an indication of at least an approach to equilibrium in the experiments. Second, there is an obvious systematic decrease in the anorthite component of plagioclase with increasing pressure. This shift varies with bulk composition, being 1.0%/kbar for 500B (anorthosite) and somewhat higher for the mafic compositions. Also, this shift occurs in plagioclase with a negligible orthoclase component (500B, HLCA), as well as in plagioclase with a modest orthoclase component (Or_{4-5} in TJ), and so the shift is primarily due to a change in the Ab/An ratio. The fact that these are near-liquidus experiments with plagioclase as the sole silicate phase (there are traces of sulfide in some of the TJ experiments) is especially significant because the liquid composition is nearly constant over the range in pressure, and the change in plagioclase composition results from a change in plagioclase-liquid partitioning along the liquidus. We emphasize that these results apply only to anhydrous systems because there is definitive experimental work showing that plagioclase along the liquidus becomes increasingly anorthitic with increasing H_2O pressure (e.g., Housh and Luhr, 1991).

Previously, Green (1969) observed shifts to more al-

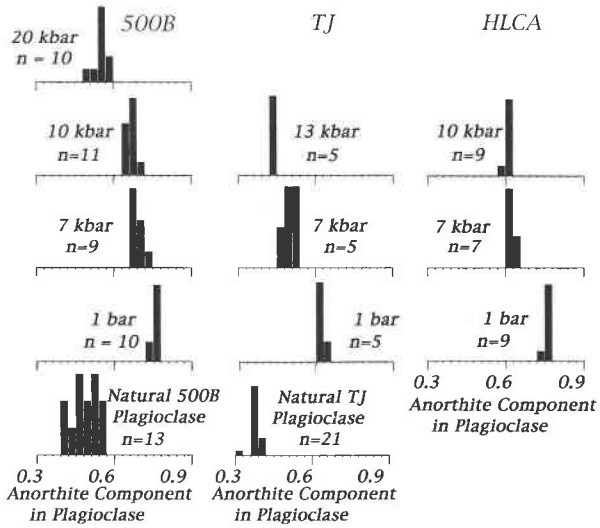

Fig. 1. Frequency distributions of plagioclase compositions in samples from massif anorthosite complexes and in near-liquidus experiments at various pressures. See text for sample descriptions. The vertical scale in each histogram is varied so that all histograms have the same height; *n* refers to the number of analyses in each plot.

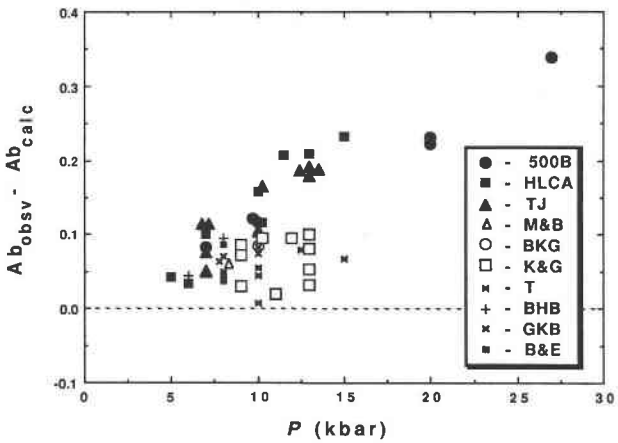

Fig. 2. Pressure vs. the difference in plagioclase composition (Ab mole fraction) between values measured in high-pressure melting experiments and values predicted by the Drake (1976) model for the temperature and liquid composition of each experiment. Solid symbols are published (HLCA, 500B: Fram and Longhi, 1992) and unpublished data (TJ) from this laboratory; other symbols are from the literature: B&E = Baker and Eggler (1987); BHB = Bender et al. (1978); BKG = Bartels et al. (1991); GKB = Grove et al. (1992); K&G = Kinzler and Grove (1992); M&B = Mahood and Baker (1986); T = Thy (1991).

bitic plagioclase in a variety of compositions from andesite to high-Al basalt to gabbroic anorthosite. Our work extends the range to more anorthositic (500B) and more ferroan and potassic (TJ) compositions. Since Green (1969), others have observed a similar change in plagioclase-liquid partitioning with increasing pressure in the presence of other phases in anhydrous, subliquidus experiments: Green et al. (1979) noted the effect in MORB compositions, Mahood and Baker (1986) in mildly alkalic basalt from Pantelleria, and Thy (1991) in mildly alkalic basalt from Iceland. Thus the change in plagioclase-liquid partitioning that produces more albitic plagioclase with pressure is apparently a general feature of anhydrous natural basaltic systems. However, increasing pressure along the liquidus is accompanied by increasing temperature, and the possibility also exists that the partitioning behavior is compositionally dependent, and so it would be useful to separate and quantify the effects of temperature, pressure, and composition. To this end we have derived empirical correction factors for several existing anhydrous plagioclase-liquid models (Ariskin and Barmina, 1990; Drake, 1976; Weaver and Langmuir, 1990) by comparing plagioclase compositions produced in liquidus and subliquidus high-pressure experiments with the plagioclase compositions at low pressure predicted by these models.

Figure 2 illustrates the difference in composition of experimental plagioclase and plagioclase calculated from the Drake (1976) model at 1 bar vs. actual pressure [results for the Weaver and Langmuir (WL) and the Ariskin and Barmina (AB) models are similar]. The difference between the observed and calculated albite fraction in liquidus and subliquidus plagioclase is a nearly linear function of pressure for the Lamont-Doherty (L-D) data (solid symbols). The pressure dependence of this difference is nearly the same as that observed along the liquidus (Fig. 1), which implies that temperature and composition, which are accounted for by the model calculations, have only minor contributions to the shift to more albitic plagioclase. Computed differences in plagioclase composition for several data sets from the literature also fall close to the L-D trend: Baker and Eggler (1987), high-Al basalt; Bartels et al. (1991), high-Al basalt; Bender et al. (1978), MORB; Grove et al. (1992), MORB; and Mahood and Baker (1986), mildly alkalic basalt. However, two data sets lie conspicuously off the L-D trend: Kinzler and Grove (1992), transitional to strongly nepheline-normative lherzolite melts; and Thy (1991), mildly alkalic basalt. These latter sets of liquids are more nepheline normative and have higher values of Mg′ [MgO/(MgO + FeO), molar] than the others. Yet, as mentioned above, Thy (1991) noted a significant pressure dependence in Ab-An partitioning among his plagioclase-liquid pairs. Although there may be some coupling of composition and pressure effects, we believe that the offsets of the Kinzler and Grove (1992) and Thy (1991) data sets are primarily the result of simple compositional effects that the empirical model of Drake (1976), based entirely on hypersthene-normative compositions with lower Mg′, does not fully describe.

A complete plagioclase-liquid partitioning model awaits production of plagioclase-liquid pairs over a much wider range of composition than exists, particularly if one excludes low-pressure experiments that may have undergone partial volatilization of alkalis. In the interim, how-

ever, using multiple regression techniques, we have computed empirical adjustments to the existing plagioclase-liquid models for the high-pressure data set shown in Figure 2. This data set excludes experiments lasting 6 h or less (e.g., Green, 1969) and experiments with the basalt-sandwich configuration (e.g., Stolper, 1980), which are prone to incomplete equilibration (Kinzler and Grove, 1992). We have also excluded the data of Meen (1990). His data set contains some liquid compositions that are generally similar to the rest of the high-pressure data, yet coexisting plagioclase is distinctly more anorthitic, and inclusion of the Meen data markedly reduced the goodness of fit regardless of which set of compositional variables was employed. Meen (1990) used Pt capsules presaturated with Fe and imposed an initial oxidation state at the Ni-NiO buffer on his starting materials; Fe loss to the capsule during the experiment increased the oxidation state further. In contrast, all of the other plagioclase-liquid pairs were produced in graphite capsules, which impose an f_{O_2} that is at least two orders of magnitude more reducing than Ni-NiO at 10 kbar (Holloway et al., 1992). Why differences in oxidation state should affect Ab-An partitioning between plagioclase and liquid is not clear, especially since the Fe concentrations in Meen's plagioclase analyses do not appear to be unusually high; however, the expressions that follow may not apply under highly oxidized conditions. Another possibility is that the plagioclase, more anorthitic than expected, results from contamination of Meen's experiments with H_2O inasmuch as H_2O pressure changes Ab-An partitioning in the opposite direction of anhydrous pressure (Housh and Luhr, 1991).

We have used stepwise multiple regression techniques (Draper and Smith, 1966) to compute correction factors for the models of Ariskin and Barmina (1990), Drake (1976), and Weaver and Langmuir (1990). These are listed in Table 1. The revised models have the form

$$\ln K^{\text{plag-liq}}\,(\text{new}) = \ln K^{\text{plag-liq}}\,(\text{old}) + A_1X_1 + A_2X_2 + A_3X_3 + A_4X_4 + \ldots \quad (1)$$

where the A terms are regression constants and the X terms are the variables P/T, $1/T$, and assorted compositional terms as discussed below. The Drake and AB models have complex partition coefficients of the form

$$K_{\text{Ab}}^{\text{plag-liq}} = \frac{\text{NaAlSi}_3\text{O}_8^{\text{plag}}}{\text{NaAlO}_2^{\text{liq}} \cdot (\text{SiO}_2^{\text{liq}})^3} \quad (2)$$

and

$$K_{\text{An}}^{\text{plag-liq}} = \frac{\text{CaAl}_2\text{Si}_2\text{O}_8^{\text{plag}}}{\text{CaAl}_2\text{O}_4^{\text{liq}} \cdot (\text{SiO}_2^{\text{liq}})^2} \quad (3)$$

where $\text{NaAlSi}_3\text{O}_8^{\text{plag}}$ and $\text{CaAl}_2\text{Si}_2\text{O}_8^{\text{plag}}$ are the atomic Na/(Ca + Na + K) and Ca/(Ca + Na + K) ratios in plagioclase, and where $\text{NaAlO}_2^{\text{liq}}$, $\text{CaAl}_2\text{O}_4^{\text{liq}}$, and $\text{SiO}_2^{\text{liq}}$ are the mole fractions of the two-lattice components for the Bottinga and Weill (1972) liquid model employed by Drake (1976) and the Nielsen and Dungan (1983) model employed by Ariskin and Barmina (1990).

For the WL model, we have only calculated a correction to the logarithm of the effective exchange coefficient (K_d) for the predicted An component. In the WL model the individual equations are not designed to produce independent estimates of the Ab and An components. Rather, Weaver and Langmuir advocated an iterative scheme of first calculating individual An and Ab components with an estimated temperature and then adjusting the temperature in subsequent calculations until Ab + An = 1.0. In this way temperature and plagioclase composition are coupled. However, for our calculations, the temperature is known for the experiments, so the plagioclase composition is obtained directly by normalizing the calculated Ab and An components together with the observed orthoclase component. We then used the calculated An component in plagioclase and the anorthite component in the liquid to compute an exchange coefficient for the anorthite component:

$$K_{d\text{An}}^{\text{plag-liq}} = \frac{(1 - \text{An}^{\text{plag}}) \cdot \text{An}^{\text{liq}}}{(1 - \text{An}^{\text{liq}}) \cdot \text{An}^{\text{plag}}} \quad (4)$$

where An^{liq} is the fraction of anorthite in the normative (molecular) feldspar. This formulation assumes equal mixing of Ab and Or components, an approximation that will produce negligible errors in basaltic plagioclase. In order to avoid the artificial effects on the normative feldspar composition caused by calculating normative feldspathoids or free wollastonite in undersaturated liquids, negative silica is ignored and the low-silica components in the norm are not calculated.

The choice of variables in the multiple regression calculations is based in part on thermodynamic formalisms and in part on petrologic intuition. The temperature and pressure dependence of an equilibrium constant (K_{eq}) is given by

$$-RT \ln K_{eq} = \Delta H^0 - T\Delta S^0 + P\Delta V^0. \quad (5)$$

The K_{Ab} and K_{An} terms employed by Drake (1976) are approximations of equilibrium constants, and so may be represented as

$$\ln K_{\text{Ab}}^{\text{xtal-liq}} = \frac{A}{T} + \frac{BP}{T} + C \quad (6)$$

where A, B, and C are enthalpy, volume, and entropy terms, respectively. Thus it is possible to modify the existing low-pressure models simply by introducing a P/T term. However, as mentioned above, the Drake (1976), AB, and WL models were constructed from data sets that do not span the entire compositional range of the high-pressure data set, and so unless the various activity terms work perfectly, there will be residual compositional and, possibly, thermal dependencies that are not accommodated. For example, the AB data set includes nepheline-normative compositions but does not incorporate the

TABLE 1. Adjustments to plagioclase-liquid partitioning models

Model	Qtz³	P (bars)/T (K)	Qtz	$10^4/T$ (K)	An^{liq}
K_{Ab}*	−15.895 ± 5.193 (0.684)	0.0496 ± 0.0050 (0.671)	8.6214 ± 2.4304 (0.670)	−0.4306 ± 0.0908 (0.571)	0.6789 ± 0.1831 (0.305)
K_{An}*		0.0339 ± 0.0116 (0.192)		−0.1773 ± 0.0454 (0.766)	−1.2179 ± 0.3769 (0.019)
K_{Ab}**	−38.605 ± 3.218 (0.533)	0.0733 ± 0.0073 (0.589)	21.581 ± 1.5024 (0.703)	−0.9162 ± 0.0580 (0.096)	
$K_{d_{An}}$†	4.8160 ± 1.6264 (0.521)	0.0585 ± 0.0124 (0.618)	−0.4755 ± 0.3604 (0.538)		
K_{An}§					

Note: Values were calculated using ln K (new) = ln K (old) + Δ, where $\Delta = A_1Qtz^3 + A_2P/T + A_3Qtz + A_4 10^4/T + A^5An^{liq} + A_6Or^{liq} + A_7Mg'$. Qtz = $(2SiO_2 + Al_2O_3 - FeO_{tot} - MgO - MnO - CaO - 5K_2O - 5Na_2O)/(2SiO_2 + 5Al_2O_3 + FeO + MgO + MnO - CaO - K_2O - Na_2O)$; $An^{liq} = (Al_2O_3 - K_2O - Na_2O)/(Al_2O_3 + K_2O + Na_2O)$; $Or^{liq} = 2K_2O/(Al_2O_3 + Na_2O + K_2O)$; $Mg' = MgO/(MgO + FeO)^{liq}$. R^2 is the multiple correlation coefficient (multiple regression with no intercept); ± = standard error of estimate for each variable; ( ) = R, simple correlation coefficient (regression with intercept).

* Drake (1976): $K_{Ab} = NaAlSi_3O_8^{plag}/[NaAlO_2^{liq}(SiO_2^{liq})^3]$, $K_{An} = CaAl_2Si_2O_8^{plag}/[CaAl_2O_4^{liq}(SiO_2^{liq})^2]$ with Bottinga and Weill (1972) liquid components.

** Ariskin and Barmina (1990): $K_{Ab} = NaAlSiO_8^{plag}/[NaAlO_2^{liq}(SiO_2^{liq})^3]$ with modified Bottinga-Weill components after Nielsen and Dungan (1983).

† Weaver and Langmuir (1990): $K_{d_{An}} = (1 - An^{plag})/(1 - An^{liq})(An^{liq})/An^{plag}$, where An^{plag} is calculated by the method described in the text.

‡ Av. $(An_{calc}\text{-}An_{obs})$ for WL and Grove et al. (1992) models.

§ Grove et al. (1992).

highly aluminous liquid compositions of this study, whereas the Drake and WL data sets include neither highly aluminous nor nepheline-normative liquid compositions. Therefore, in addition to a P/T variable, we have also included $1/T$ and compositional variables in the regression calculations.

As a guide for choosing activity-composition terms, we note that mixing of components in the liquid is likely to depend upon liquid structure, which in turn depends upon the extent of the Si-tetrahedral network and the proportions of the various large cations, whereas mixing in plagioclase will depend on the proportions of the Ab, Or, and An components. To account for compositional variation in the liquid, we have chosen Mg′ and the Qtz and La fractions in the O units of the model quarternary system of Pan and Longhi (1990) containing olivine (Ol), larnite (La), nepheline, calcium aluminate (Ne,CA), and free silica (Qtz). We prefer free silica and Ca components to simple oxides because these components remove some of the coupling of elements (Na-Al, Ca-Al) that is likely to occur. Given that the extent of network polymerization is not a simple function even of free SiO_2 concentration (Hess, 1980), we have also included Qtz^3 as a possible variable. To model feldspar activities, An^{liq} and Or^{liq} are included in the regression because plagioclase composition will vary in response to changes in feldspar components in the liquid. This approximation makes it possible to calculate the partition coefficient in one step without prior knowledge of the plagioclase composition and, hence, greatly simplifies the computation.

The stepwise regression procedure first ranks all the variables in order of their individual correlation coefficients and then checks each new variable for statistical significance at the 95% confidence level. This procedure tends to eliminate not only extraneous variables, but also less significant variables that correlate with other stronger variables. The order of the variables in Table 1 is the initial ranking for the Drake (1976) model. The fact that the set of significant variables is different in each modified model is a reflection of each low-pressure model accounting for compositional variation differently. The last column in Table 1 also contains a test of each modified model against the 55 plagioclase-liquid pairs in the data base reported as the average difference and standard deviation between calculated and observed albite fraction.

Results of the regression show that the pressure dependence of An partitioning is less than that of Ab partitioning and much weaker statistically. The modified Drake (1976) model for Ab reproduces plagioclase compositions better than the An model (±0.03 vs. ±0.10). This disparity was noted previously by Drake (1976) and Langmuir (personal communication) at 1 atm and suggests some activity-composition relation not accounted for by any of the modeling. The modified Drake model for Ab reproduces the high-pressure data set not only better than the modified AB and WL models, but also better than the Grove et al. (1992) model, which we have not modified but which contains a pressure term.

To test the possibility that Or variations in plagioclase might be affecting An partitioning, a regression of ln K_{Or} was conducted against the variable set in Table 1, where K_{Or} has a form analogous to Equation 2. The results (not tabulated) show that no variable correlates well with K_{Or} (the highest individual R is only 0.45), and even multiple variables provide a weak fit ($R^2 = 0.38$).

Given that the prediction of Ab appears more precise than that of An and that K_{Or} does not correlate well with plausible compositional parameters, we suggest that the modified Drake model be employed only to calculate the Ab component. The proportions of the An and Or components may then be calculated in the following way. Because the Or component is minor in basaltic plagioclase, its concentration can be estimated with little uncertainty by means of a simple partition coefficient, and the An component can then be obtained by difference. The average molar plagioclase partition coefficient for K_2O ($D^{*plag\text{-}liq}_{K_2O}$—here we adopt the convention of Beattie et al., 1993) in the subset of 45 high-pressure plagioclase-liquid pairs with K_2O in plagioclase ≥0.05 wt% is 0.36 ± 0.10. The Or component in plagioclase is thus

$$KAlSi_3O_8^{plag} = 0.36K_2O^{liq}/0.125 \quad (7)$$

TABLE 1.—*Continued*

Model	Or^{liq}	Mg′	R^2	Av. (Ab_{calc}-Ab_{obs})
K_{Ab}*	2.0294 ± 0.4838 (0.081)	−0.5406 ± 0.1734 (0.075)	0.884	0.0009 ± 0.0291
K_{An}*	1.1656 ± 0.9687 (0.341)	2.1721 ± 0.4739 (0.331)	0.472	0.0007 ± 0.1008
K_{Ab}**			0.912	−0.0025 ± 0.0490
$K_{d_{An}}$†			0.493	0.0005‡ ± 0.0474
K_{An}§				−0.066‡ ± 0.074

where 0.125 is the mole fraction of K_2O in the Or component.

Low-Ca pyroxene-liquid

Orthopyroxene megacrysts from anorthosite massifs typically have compositions different from the smaller matrix orthopyroxenes that presumably crystallized at the level of emplacement. The contrast is especially apparent for Al_2O_3 concentrations as shown in Figure 3 with data from Harp Lake and elsewhere (Emslie, 1980). The megacrysts have exsolved augite and plagioclase lamellae, and the compositions in Figure 3 are from bulk or integrated analyses. The matrix pyroxenes all have exsolved augite lamellae too, but Al_2O_3 concentrations in the exsolved crystals are probably not significantly different from the original concentrations. We base this interpretation on the one integrated matrix composition, which indicates the approximate CaO content of the original orthopyroxenes, plus the shallow slopes of mixing vectors originating at orthopyroxene hosts and pointing toward the compositions of their associated lamellae. Fram and Longhi (1992, their Fig. 5) showed that orthopyroxenes coexisting with liquid and intermediate plagioclase in the range of 5–11.5 kbar in isobaric experiments on HLCA (high-Al gabbro) had compositions very similar to those of natural megacrysts from various anorthosite massifs. In particular, the Al_2O_3 concentrations in the experimental orthopyroxenes increased systematically with pressure (Fig. 3), suggesting that the various megacrysts crystallized (or recrystallized?) over depths ranging from ~10 to >35 km. In order to establish this hypothesis more firmly, we have attempted to reverse orthopyroxene compositions produced in the isobaric experiments. Also, even though HLCA is a plausible parent magma composition for the Harp Lake anorthosites, it is useful to establish some general compositional controls on Al_2O_3 partitioning between orthopyroxene and liquid, so as to interpret correctly Al_2O_3 concentrations in megacrysts from other complexes where the parent magma may have been somewhat different.

Figure 4 shows the results of two sets of reversal experiments where individual spot analyses of orthopyroxene from the polybaric experiments are contrasted with the average orthopyroxene analyses of the isobaric experiments reported by Fram and Longhi (1992). Table 2 lists analyses and experiment conditions. Figure 4a clearly shows a bimodal distribution of points with analyses of cores overlapping the range of analyses from the 6-kbar isobaric experiment and analyses of rims overlapping the range of analyses from the 11.5-kbar experiment. Figure 4b shows a single cluster of points partially overlapping the range of analyses from the 6-kbar isobaric experiment and no trace of relict compositions from the first stage of

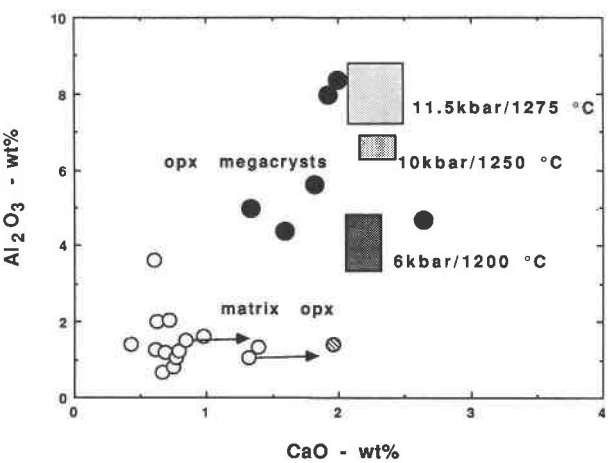

Fig. 3. Al_2O_3 and CaO concentrations (weight percent) in orthopyroxenes. Open circles: spot analyses of exsolved matrix orthopyroxenes from the Harp Lake Complex; shaded circle: integrated composition of orthopyroxene host with augite lamellae from Harp Lake; vectors indicate mixing paths between orthopyroxene hosts and augite lamellae; solid circles: bulk and integrated orthopyroxene megacryst compositions from Harp Lake and other massif anorthosite complexes; shaded boxes show 1 sd about average orthopyroxene compositions from experiments on HLCA. All natural compositions from Emslie (1980); experimental data from Fram and Longhi (1992). Note the experiment at 1200 °C, 6 kbar (HLCA-8) was erroneously reported as having been performed at 7 kbar.

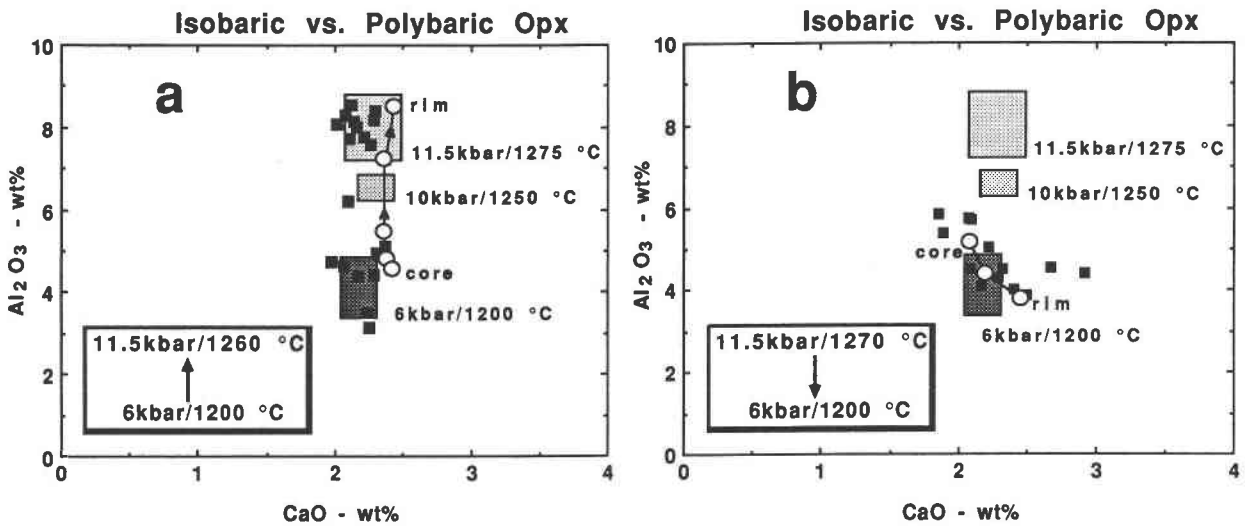

Fig. 4. Comparison of average compositions of orthopyroxenes produced in isobaric melting experiments on HLCA (shaded boxes as in Fig. 3), with spot analyses of orthopyroxenes produced in polybaric experiments. Solid squares = random spot analyses; open circles = core to rim traverses of single crystals, with arrows indicating direction of rim. (**a**) Stage 1 at low pressure, stage 2 at high pressure; (**b**) stage 1 at high pressure, stage 2 at low pressure.

the experiment. The data in Figure 4a are unequivocal evidence of a reversal in composition. The data in Figure 4b are subject to two interpretations: either reaction of the high-Al_2O_3, high-pressure cores went nearly to completion, or the high-pressure pyroxenes were not present when final P/T conditions were achieved in the second stage (examination of a small chip of material from the first stage of the experiment shows that aluminous orthopyroxene was present, and so either the remainder of the pyroxene-bearing portion of the first stage was lost in reloading the capsule for the second stage, or in the second stage temperature cycled briefly above the experiment temperature and all the pyroxene melted). We believe that the reaction went nearly to completion, but in either case the data in Figure 4a are sufficient to demonstrate that increasing Al_2O_3 in orthopyroxene coexisting with plagioclase-saturated liquid is an equilibrium effect of increasing pressure.

Two factors contribute to increasing Al_2O_3 concentration in orthopyroxene with pressure: one is the influence of pressure on the pyroxene and liquid atomic structures in facilitating incorporation of aluminous components,

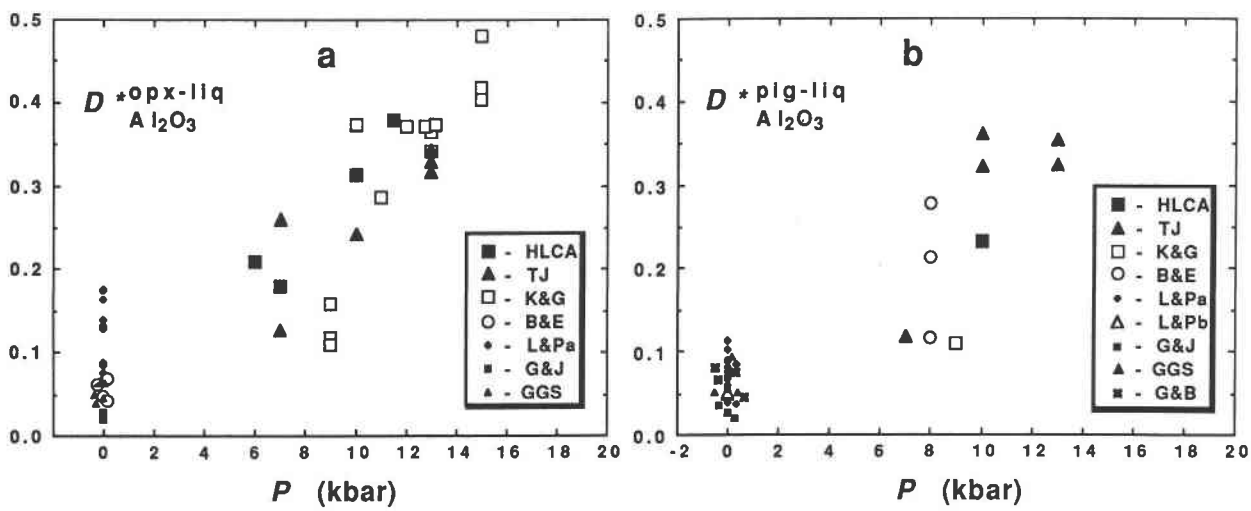

Fig. 5. Variation with pressure of simple molar partition coefficient for Al_2O_3 between low-Ca pyroxene and liquid. (**a**) Orthopyroxene-liquid pairs; (**b**) pigeonite-liquid pairs. Symbols: B&E = Baker and Eggler (1987); GGS = Grove et al. (1982); G&B = Grove and Bryan (1983); G&J = Grove and Juster (1989); K&G = Kinzler and Grove (1992); L&Pa, L&Pb = Longhi and Pan (1988, 1989, respectively); HLCA data from Fram and Longhi (1992); TJ data are unpublished.

TABLE 2. Compositions of pyroxene and liquid in reversal experiments

	HLCA-55*					HLCA-53**			
	Liq[5]	Opx Core	Opx Mantle	Opx Mantle	Opx Rim	Liq[4]	Opx Core	Opx Mantle	Opx Rim
SiO_2	48.8(3)	52.7	52.0	51.1	50.5	48.1(3)	52.4	53.0	53.3
TiO_2	2.59(1)	0.34	0.31	0.20	0.20	2.74(5)	0.88	0.84	0.85
Al_2O_3	17.2(1)	4.45	5.48	7.73	8.55	15.4(9)	5.05	4.28	3.79
Cr_2O_3	0.14(2)	0.20	0.25	0.36	0.26	0.15(2)	0.33	0.28	0.35
FeO_{tot}	12.1(2)	15.0	15.0	14.3	14.1	12.7(1)	14.8	14.8	14.7
MgO	5.56(5)	25.2	24.8	24.9	24.2	5.94(5)	24.9	25.3	25.5
MnO	0.29(3)	0.28	0.19	0.17	0.22	0.34(1)	0.38	0.42	0.39
CaO	8.43(3)	2.28	2.35	2.10	2.42	8.41(7)	2.22	2.29	2.47
K_2O	0.67(4)					0.69(9)			
Na_2O	3.06(16)	0.12	0.15	0.11	0.20	3.56(7)	0.15	0.15	0.14
P_2O_5	0.39(2)					0.40(1)			
Total	99.2	100.4	100.5	101.0	100.6	98.4	101.1	101.4	101.5

Note: [ ] = no. of point analyses in average; ( ) = 1 sd of average analyses in terms of the least units cited.
* HLCA-55: 67 h at 1200 °C and 6 kbar → 119 h at 1260 °C and 11.5 kbar (+ plag).
** HLCA-53: 72 h at 1270 °C and 11.5 kbar → 116 h at 1200 °C and 6 kbar (+ plag, ol).

such as $MgAl_2SiO_6$, in pyroxene; the other is the shift in the orthopyroxene-plagioclase liquidus boundary to more aluminous compositions (e.g., Sen and Presnall, 1984). These two effects lead to different patterns of variation of the molar partition coefficient for Al_2O_3 between orthopyroxene and natural basaltic liquid, $D^{*\text{opx-liq}}_{Al_2O_3}$, as a function of pressure. If D^* remains constant with pressure, then all of the increase in Al_2O_3 concentration in pyroxene with pressure results from the shift in the orthopyroxene-plagioclase liquidus boundary to more aluminous compositions; if D^* increases by the same relative amount as the absolute Al_2O_3 concentration in pyroxene, then all the increase in Al_2O_3 is due to structural effects. Figure 5a shows that there is a marked increase in $D^{*\text{opx-liq}}_{Al_2O_3}$ with pressure, both in our data and in recent data from the literature. The data show that the relative increase in D^* for HLCA between 6 and 11.5 kbar (a factor of 2.1) is approximately 90% of the relative increase in the Al_2O_3 concentration in pyroxene (a factor of 2.3). Thus most of the pressure effect on Al_2O_3 in orthopyroxene is structural. Figure 5b indicates a similar situation for pigeonite.

Even though most of the variation in D^* is accounted for by pressure, additional compositional controls on D^* are likely. These controls may be predicted by examination of the crystal-liquid equilibria that describe Al_2O_3 substitution. Consider the formation of the Mg-Tschermak's component from oxides:

$$\underset{\text{liquid}}{MgO} + \underset{\text{liquid}}{Al_2O_3} + \underset{\text{liquid}}{SiO_2} = \underset{\text{orthopyroxene}}{MgAl_2SiO_6}. \quad (8)$$

The familiar expression for the equilibrium constant may be rearranged as

$$\ln \frac{a^{\text{opx}}_{MgAl_2SiO_6}}{a^{\text{liq}}_{Al_2O_3}} = \ln K_8 + \ln a^{\text{liq}}_{MgO} + \ln a^{\text{liq}}_{SiO_2} \quad (9)$$

where a_i is the activity of component i. Given $a_i = \lambda_i X_i$ and $X^{\text{opx}}_{Al_2O_3} = 0.333 X^{\text{opx}}_{MgAl_2SiO_6}$, where λ_i and X_i are the activity coefficient and mole fraction of component i, respectively, and where 0.333 is a stoichiometric coefficient, it is possible to obtain an expression for the partition coefficient by substitution in the left side of the equation:

$$\ln D^{*\text{opx-liq}}_{Al_2O_3} = \ln \frac{X^{\text{opx}}_{Al_2O_3}}{X^{\text{liq}}_{Al_2O_3}}$$
$$= \ln K_8 + \ln a^{\text{liq}}_{MgO} + \ln a^{\text{liq}}_{SiO_2} + \ln \lambda^{\text{liq}}_{Al_2O_3} - \ln \lambda^{\text{opx}}_{MgAl_2SiO_6} + \ln 0.333. \quad (10)$$

The PTX dependence of the simple molar partition coefficient for Al_2O_3 may finally be obtained by substituting for the equilibrium constant. The result is an equation in the form of Equation 6 where the C term is

$$C = \frac{\Delta \bar{S}^0_8}{R} + \ln a^{\text{liq}}_{MgO} + \ln a^{\text{liq}}_{SiO_2} + \ln \lambda^{\text{liq}}_{Al_2O_3} - \ln \lambda^{\text{opx}}_{MgAl_2SiO_6} + \ln 0.333. \quad (11)$$

If Equation 8 were written in terms of cation units (i.e., $AlO_{1.5}$) and if site occupancies were employed to model pyroxene activities, the right side of Equation 10 would have a different stoichiometric coefficient term, ln 0.25, and all the terms would be divided by 2. Thus even though D^* expressed in cation units would have a somewhat different value, the PTX dependencies of ln D^* would differ only by constants, and so there would be no practical advantage to using cation units in the regression analysis of ln D^* that follows.

As the derivations of corrections to plagioclase-liquid models above illustrate, more complicated two-lattice activity models do not completely account for compositional variations. Also, two-lattice models erroneously predict unit silica activities in all Al-free liquids, so their adequacy in relating silica activities in plagioclase-saturated and -undersaturated liquids is suspect. Consequently, we have not employed two-lattice models. Since there are no simple expressions for oxide activities or activity coefficients in silicate liquids, we have chosen various simple approximations. However, there is an additional problem because some of the Al in pyroxene may be as-

TABLE 3. Pressure, temperature, and composition dependence of the simple molar partition coefficient for Al_2O_3 between low-Ca pyroxene and liquid

A_0	P (bars)/T (K)	ln(Qtz)	$10^4/T$ (K)	ln(FMO)	Wo^{pyx}
		$\ln D^{*opx-liq}_{Al_2O_3}$			
−3.8538 ± 0.5190	0.1473 ± 0.0334 (0.856)	−1.3680 ± 0.6346 (0.826)	(0.587)	(0.377)	(0.321)
		$\ln D^{*pig-liq}_{Al_2O_3}$			
−11.6758 ± 3.7591	0.2306 ± 0.0330 (0.830)	−1.1732 ± 0.6119 (0.512)	1.1313 ± 0.4593 (0.384)	(0.107)	(0.444)

Note: ln $D^* = A_0 + x_1A_1 + x_2A_2 + x_3A_3 + \ldots$; Qtz as in Table 1; FMO = FeO_{tot} + MgO + MnO (mole fractions); Wo^{pyx} = CaO/(CaO + MgO + FeO_{tot}); X(Na + K) = Na_2O + K_2O (mole fractions); $XTiO_2$ = TiO_2 (mole fraction); Mg′ as in Table 1; R^2 is the multiple correlation coefficient; av. Δ is the average deviation in the predicted D^*; ± = standard error of estimate for each variable; ( ) = simple correlation coefficient.

sociated with Fe- and Mn-Tschermak's components as well as Mg-Tschermak's. Furthermore, Al is unlikely to be distributed proportionately among these components. Accordingly, the regression includes terms for total MgO + FeO + MnO and for Mg-Fe exchange (Mg′) in the liquid (Mg′ in the liquid will reflect Mg′ in pyroxene). The same O-based, free silica component (Qtz) as above is employed for silica activity, and because Al may be closely coupled with alkalis in the tetrahedral network of silicate liquids (Bottinga and Weill, 1972), a term for total alkalis is included. The activity coefficient for Mg-Tschermak's component may also depend on the wollastonite content of the pyroxene, so we have included a term for Wo^{pyx}. Finally, not all the Al in basaltic pyroxene is going to form a tschermakitic component. Some will form an $NaAlSi_2O_6$ (jadeite) component; however, the total alkali term just mentioned accommodates this possibility in liquids with low to moderate K_2O concentrations. Also, some Al will also form an $R\text{TiAl}_2O_6$ component (where R may be Mg, Fe, Mn, or Ca). As with other components, since $R\text{TiAl}_2O_6$ in pyroxene will reflect TiO_2 in the liquid, we have included a term for TiO_2 concentration in the liquid.

Table 3 contains the results of the stepwise multiple regression. The variables are listed in order of their individual correlations with ln $D^{*opx\text{-}liq}_{Al_2O_3}$. Not surprisingly, the P/T term was the most significant term for both the orthopyroxene and pigeonite regressions. The individual regressions show that ln Qtz (R = 0.826) correlates with ln $D^{*opx\text{-}liq}_{Al_2O_3}$ nearly as well as P/T (R = 0.856), but its correlation with ln $D^{*pig\text{-}liq}_{Al_2O_3}$ (R = 0.512) is much weaker. The reason for this disparate behavior is that Qtz varies more in the set of liquids coexisting with orthopyroxene (some high-pressure liquids are nepheline normative), and this variation tends to correlate with P/T. The strong correlations of P/T with ln D^* in both sets, whether Qtz varies strongly or weakly, indicates that P/T is the dominant control on D^*. However, in both cases ln Qtz was a statistically significant additional variable, thus indicating that ln Qtz accounts for some of the variation in D^* that is not accounted for by P/T. Terms for TiO_2 and total alkalis in the liquid were minor but statistically significant in both regressions, whereas terms for ln(FeO + MgO + MnO) and Wo^{pyx} were not significant in either one. Mg′ and $1/T$ were significant variables only in the pigeonite-liquid regression. A free Ca component, i.e., La (Pan and Longhi, 1990), in the liquid, used instead of Wo^{pyx}, was not a significant variable either. These results indicate that pressure is the dominant control on Al partitioning between low-Ca pyroxene and liquid, that silica activity appears to have a secondary control, but temperature and other compositional controls are relatively minor.

DISCUSSION

The data presented here are generally consistent with the hypothesis that the bulk of the plagioclase in massif anorthosites plus the most aluminous orthopyroxene megacrysts crystallized from a high-Al basaltic magma (e.g., HLCA) at relatively high pressures (9–15 kbar) and then were carried upward in diapiric mushes or crystal-rich suspensions. However, there are several aspects of the hypothesis that need further examination, such as plagioclase reequilibration, the possible role of kinetics in producing aluminous pyroxene, and magma dynamics.

Plagioclase reequilibration and mass balance

Despite the generally massive appearance of most true anorthosites, there is abundant evidence of silicate liquid at the level of emplacement in the form of rhythmic layering and mesocumulus textures in rocks with higher proportions of olivine or pyroxene (e.g., Emslie, 1980; Duchesne, 1984; Scoates and Lindsley, 1989; Wiebe, 1990). A question immediately arises: why doesn't the plagioclase that crystallized at high pressure but later is surrounded by liquid at lower pressure reequilibrate to more anorthitic compositions or at least develop strong reverse zoning? Many plagioclase crystals in anorthosites do indeed have very thin reversely zoned rims (Emslie, 1980; unpublished data from this lab), but such rims are volumetrically insignificant and also appear to be a general feature of mafic plutonic rocks with cumulus plagioclase, where they appear to be related to in situ crystallization of interstitial liquid (Morse and Nolan, 1984) and thus may have no direct bearing on the anorthosite problem. Rather, the answer to the question may lie in a combination of slow cooling and mass balance effects, as illustrated in Figure 6.

Figure 6 schematically illustrates the effect of pressure on tie lines between plagioclase and liquid. Increasing pressure produces a more albitic plagioclase coexisting with a given liquid, and hence high-pressure tie lines are

TABLE 3.—*Continued*

$X(Na + K)$	$XTiO_2$	Mg′	R^2	Av. Δ
		$\ln D^{*\,opx\text{-}liq}_{Al_2O_3}$		
−1.3196 ± 3.7585 (0.266)	15.361 ± 5.7774 (0.152)	(0.015)	0.821	0.007 ± 0.057
		$\ln D^{*\,pig\text{-}liq}_{Al_2O_3}$		
−7.3696 ± 4.8560 (0.500)	5.8184 ± 6.1299 (0.494)	0.1262 ± 0.7617 (0.612)	0.856	−0.007 ± 0.040

steeper than low-pressure tie lines (compare 12-kbar tie line *aa′* with 3-kbar tie line *aa″*). Equilibrium requires a tie line to rotate through the bulk composition of a crystal + liquid mixture following a change in pressure. Accordingly, a parent magma derived from depth with only a few high-pressure plagioclase phenocrysts will encounter a strong tie line rotation with respect to plagioclase composition because the tie line joining plagioclase and liquid will rotate about a point close to the liquid composition. Consequently, plagioclase (~*a″*) that is markedly more anorthitic than the phenocrysts (*a′*) will crystallize at low pressures, and the high-pressure crystals will either tend to dissolve or will develop strongly reversed zoning. On the other hand, during decompression of a crystal-rich suspension, very limited rotation of the tie line with respect to plagioclase composition is possible through the bulk composition under equilibrium conditions, and so relatively little regression to more anorthitic plagioclase (*a′* → *b′*) will occur. At the same time, the tie-line rotation produces a relatively large increase in the normative albite component of the liquid (*a* → *b*). So even if the equilibrated interstitial liquid separates from the crystals at the level of emplacement, the liquid continues to precipitate plagioclase that is less anorthitic than the plagioclase crystallized from the original parent magma containing only a few phenocrysts. In fact, this separated liquid will have a greater tendency to fractionate and produce more albitic plagioclase than liquid with the same composition that remains trapped in the mush. Thus, in a series of intrusions with varying proportions of suspended high-pressure plagioclase, there is considerable capacity for a common basaltic parent magma to produce a wide range of plagioclase compositions. This analysis presupposes extensive reequilibration between plagioclase and liquid—something that is not commonly observed in the erupted products of subvolcanic magma chambers but is more likely in slowly cooled anorthositic plutons and is observed in the experiments described above on a laboratory time scale. The key to reequilibration for crystals with dimensions in millimeters may be a small amount of pressure-release melting and dissolution-reprecipitation during ascent of the mush. Plagioclase megacrysts, obviously, have escaped reequilibration or back reaction.

Does the pressure effect explain all of the difference in plagioclase composition between common basalts and massif anorthosites? Probably not. In some anorthosite complexes, such as Harp Lake (Emslie, 1980), the bulk of the plagioclase ranges from An_{50} to An_{60}, and it is not difficult to imagine that an evolved basaltic parent magma, similar to HLCA, produced these compositions while partially crystallizing at the base of the crust. There are, however, many massifs where the typical plagioclase is in the range of An_{35}–An_{50} (e.g., Anderson and Morin, 1968) and it is unlikely that only differences in the depth of ponding of a common basaltic magma such as HLCA are responsible for the entire range of typical plagioclase compositions between An_{35} and An_{60}.

Other processes that probably contribute to the characteristically intermediate plagioclase are fractional crystallization and crustal assimilation. Emslie (1985) pointed out that, in addition to being less anorthitic, plagioclase in massif anorthosites is typically enriched in Sr by a factor of two or more over plagioclase from large layered intrusions, such as the Kiglapait and Stillwater. He suggested that extensive crystallization of augite prior to the

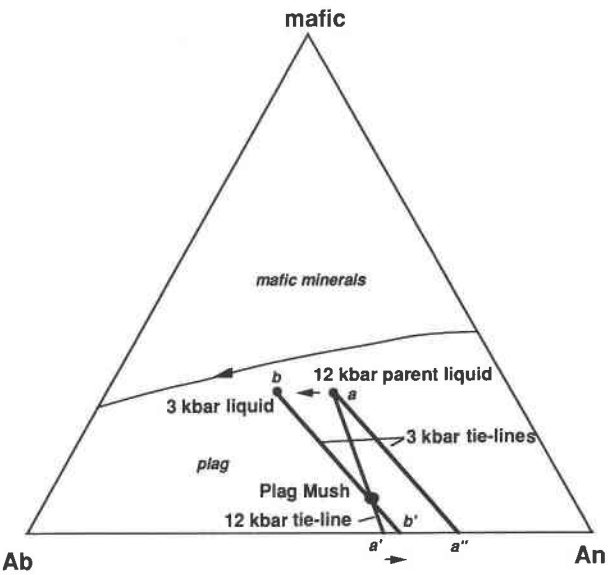

Fig. 6. Schematic representation of the relation between bulk composition of plagioclase-liquid mixtures and pressure-induced tie-line rotation: *a*-*a′* is 12-kbar tie line; *a*-*a″* and *b*-*b′* are 3-kbar tie lines. Arrows indicate direction of change in plagioclase (*a′* → *b′*) and interstitial liquid (*a* → *b*) compositions following decompression of mush from 12 to 3 kbar.

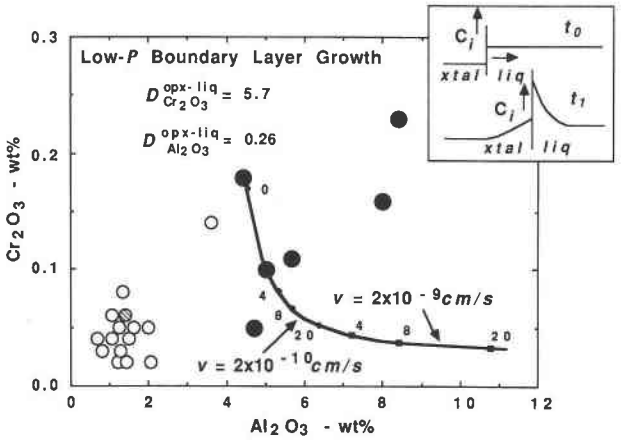

Fig. 7. Results of the solute-rejection model calculations (Smith et al., 1955) for Cr_2O_3 and Al_2O_3 incorporated into growing orthopyroxenes compared with natural matrix and megacryst compositions (symbols as in Fig. 3). Curves show the concentrations of Cr_2O_3 and Al_2O_3 in the margin of a crystal at various stages in its growth. Small numbers are the crystal diameter in centimeters. Linear crystal growth rates (2×10^{-9} and 2×10^{-10} cm/s) are taken from measurements on plagioclase in Hawaiian lava lakes by Kirkpatrick (1977). The times for crystal growth can be calculated by dividing the crystal radius divided by two by the linear growth rate. Cr_2O_3 and Al_2O_3 were assumed to have the same chemical diffusion coefficient of 10^{-8} cm^2/s^2, calculated with the algorithm of Lesher (1991). Partition coefficients are taken from experiment HLCA-8 (1200 °C, 6 kbar—note that this experiment was erroneously reported at 7 kbar by Fram and Longhi, 1992). The inset illustrates the solute rejection model for an incompatible element i: at time t_0 the crystal-liquid interface is at equilibrium; at t_1 the crystal is growing to the right at a constant rate. This model predicts zoned crystals.

crystallization of plagioclase enriched Sr and Na in the liquid while depleting Ca so as to produce the distinctive plagioclase compositions. Differences in the amount of augite fractionation might thus affect the composition of plagioclase that eventually crystallizes. In a study of several anorthositic plutons in the Nain Complex, Wiebe (1992) observed a positive correlation of An with the Mg-Fe ratio and a negative correlation of An with the Sr-Ca ratio; these correlations are consistent with Emslie's model. Given that the plagioclase liquidus field shrinks with increasing pressure (e.g., Fram and Longhi, 1992), the higher the pressure of crystallization, the more fractionation of pyroxene is possible before precipitation of plagioclase, and, hence, the less calcic the plagioclase. Thus pressure probably has a compound effect on plagioclase composition. Barker et al. (1975) argued that basaltic magmas ponded at the base of the crust not only generate anorthosites and anatectic granites but are readily contaminated as well. Assimilation of a granitic component into this ponded magma would also lead to less anorthitic plagioclase. Nd and Sr isotopic data are certainly consistent with crustal assimilation (Ashwal and Wooden, 1984). Another possibility is that the range of plagioclase compositions observed in massif anorthosites reflects a range of parental magma compositions delivered to the base of the crust. Magmas formed by smaller degrees of partial melting are likely to have higher ratios of alkalis to Ca and thus will crystallize less anorthitic plagioclase than magmas produced by larger degrees of melting. Separating the contributions from these various processes is a complicated matter that awaits identification of the primary magmas that feed the ponded chambers.

Al in orthopyroxene: Pressure vs. kinetics

The high Al_2O_3 concentrations in some orthopyroxene megacrysts have been attributed to rapid crystal growth rather than high pressure crystallization (Morse, 1975; Dymek and Gromet, 1984). This model entails in-situ growth of the megacrysts at the level of the emplacement of the anorthosites in the upper crust and, if correct, would obviate the need for a polybaric petrogenetic model. During rapid crystal growth, Al_2O_3, which partitions more readily into the liquid, builds up at the pyroxene-liquid interface faster than it can diffuse in the liquid, and the pyroxene incorporates more Al_2O_3 than it would under near-equilibrium conditions (e.g., Grove and Bence, 1977). The relative enrichment of Al_2O_3 or any other excluded element above its equilibrium concentration in the growing crystal increases as crystal growth rate and time increase and decreases as diffusivity and the partition coefficient increase. However, complementary decreases in elements that are compatible in pyroxene is an important corollary of this model.

We have tested the rapid crystal growth model using the solute-rejection equation of Smith et al. (1955) and the simple weight partition coefficients for Al_2O_3 (0.26) and Cr_2O_3 (5.7) between orthopyroxene and liquid taken from experiment HLCA-8 (1200 °C, 6 kbar) of Fram and Longhi (1992). Figure 7 shows the results of the calculations along with the Al_2O_3 and Cr_2O_3 concentrations of natural orthopyroxene megacrysts tabulated by Emslie (1980). As might be expected, the set of growth rates and times that increase Al_2O_3 concentrations in orthopyroxene to the levels observed in megacrysts also strongly deplete Cr_2O_3. Results are qualitatively similar for any choice of Al and Cr partition coefficients for orthopyroxene-liquid from the Fram and Longhi (1992) data set. In contrast, Cr_2O_3 increases along with Al_2O_3 in the natural megacrysts, and the megacrysts also have higher Cr_2O_3 concentrations than do the smaller matrix orthopyroxenes. Indeed the failure of the rapid crystal growth model is worse than it appears in Figure 7 because we chose to begin the calculation with one of the megacryst compositions for purposes of illustration rather than with one of the matrix pyroxene compositions, which would be a more appropriate departure point for the calculation. Also, rapid crystal growth should also lead to zoned crystals, as suggested in Figure 7, yet there is no evidence of zoning in the megacrysts. The presence of H_2O or other fluid components in the liquid might promote the growth of large crystals, but there is no evidence of substantially

higher concentrations of Al_2O_3 in pegmatitic orthopyroxenes from the Stillwater Complex (Boudreau, 1988) or the Bushveld Complex (Nicholson and Mathez, 1991), and so large crystals do not necessarily imply high concentrations of Al_2O_3 or even rapid crystal growth.

Another kinetic process that might be invoked to explain aluminous orthopyroxene is delayed nucleation of plagioclase in liquids that are crystallizing pyroxene. The failure of plagioclase to crystallize leads to metastable hyperaluminous liquids, which Morse (1982) suggested are parental to massif anorthosites. Such liquids would obviously crystallize more aluminous pyroxene than cotectic liquids, but the more than threefold increase in Al_2O_3 between matrix orthopyroxene and megacrysts (Fig. 7) implies physically impossible amounts of Al_2O_3 in the liquid. Furthermore, crystallization of pyroxene alone will deplete liquid of Cr_2O_3 while enriching it in Al_2O_3, thus producing a negative correlation between Cr_2O_3 and Al_2O_3, in contrast to the positive correlation observed in natural megacrysts.

One of the reasons for invoking kinetic processes to explain the aluminous megacrysts is the common occurrence of groups of orthopyroxene megacrysts intergrown with plagioclase megacrysts to form pegmatitic clots or lenses that may be several meters long (Morse, 1975; Dymek and Gromet, 1984; Duchesne and Maquil, 1992). However, the experimental evidence and calculations discussed above are inconsistent with a low-pressure origin for the megacrysts. Consequently, we believe that the large size of the megacrysts is the result of slow cooling at great depth, and we subscribe to the interpretation of Wiebe (1986) that the pegmatitic lenses are "high pressure nodules" or fragments of much more extensive orthopyroxene-plagioclase layers that were broken up and incorporated by ascending anorthositic magmas. The transport of pyroxene megacrysts in rafts of mostly crystalline layers within more mobile magma rather than as individual crystals is presumably what allows the pyroxene megacrysts to survive slow cooling at the low pressures (3–5 kbar) of final emplacement. What remains to be determined is whether the considerable range in megacryst composition (Fig. 7) reflects crystal growth from magmas ponded at various levels from the base to the middle of the crust or whether some of the megacrysts have partially reequilibrated en route to the upper crust.

Rheology

One of the major unsolved problems that polybaric models of anorthosite petrogenesis face is the feasibility of transporting plagioclase-rich suspensions or mushes from the lower to upper crust. Fram and Longhi (1992) found that, at 11.5 kbar, plagioclase and orthopyroxene coexist on the liquidus of HLCA and have compositions similar to the bulk of the plagioclase and the most aluminous orthopyroxene megacrysts of the Harp Lake Complex, respectively. The choice of a parent liquid with ~17.5 wt% Al_2O_3, such as HLCA, for massif anorthosites implies mechanical enrichment of the liquid with plagioclase to form a thick suspension or mush. From Figure 7 of Fram and Longhi (1992) it is possible to estimate crudely that 85 and 65 vol% plagioclase, respectively, must be added to HLCA to produce the average anorthosite and leuconorite (or "noritic anorthosite" according to Streckeisen, 1976) bulk compositions reported by Emslie (1980). These high proportions of crystals pose rheological problems for the transport of anorthositic magmas, presumably as diapirs (Duchesne, 1984; Longhi and Ashwal, 1984).

Miller et al. (1988) have reviewed the rheology of granitic diapirs, and many of the concerns are similar. At high degrees of crystallinity, the crystals begin to form a rigid network or "granular-framework-controlled mass" (van der Molen and Paterson, 1979), and not only does the effective viscosity of a suspension increase rapidly, but movement is possible only by shearing and deformation of the crystalline matrix. Although there is ample evidence of deformation in many anorthosites in the form of granulation, bent twinning, and stress-induced twinning, there are also large tracts of relatively undeformed, less anorthositic rocks as well, e.g., leucogabbros in the Laramie Complex (Scoates, 1992) and leuconorites in the Nain Complex (Wiebe, 1992). So there appears to be a need for transporting at least some anorthositic magma as a rheological liquid. Under nearly static conditions the transition from liquid-state to solid-state rheology or the critical melt fraction may be described in terms of contiguity. Contiguity is the fraction of the surface area occupied by solid-solid contacts (German, 1985)—in the present case, primarily plagioclase-plagioclase contacts. Miller et al. (1988) cited contiguity values of 0.15–0.2 as marking the transition. German (1985) derived a relation among contiguity, crystallinity, and wetting angle; according to his formulation the critical melt fraction lies at 0.4–0.5 for wetting angles of 45°—the angle measured for feldspar by Jurewicz and Watson (1985). German (1985) also noted a nearly 20% decrease in contiguity for a nonuniform distribution of crystal sizes. Such a decrease would lower the critical melt fraction to the range of 0.3–0.4. Recent work by Waff and Faul (1992) indicated that development of faceted crystal faces decreases the wetting angle and, hence, contiguity and the critical melt fraction still further.

Inasmuch as motion disrupts contiguity, the critical melt fraction is also a function of the shear rate of a suspension (cf. Fig. 4 of Miller et al., 1988). Experimental work by van der Molen and Paterson (1979) on partially molten granite with shear rates on the order of 10^{-5}/s has shown the transition from liquid to solid flow regimes to be at 30–35 vol% liquid, whereas other work is consistent with no transition at all. For example, the ability of suspensions to flow is often represented as effective viscosity and parameterized according to the Roscoe-Einstein model (Shaw, 1965):

$$\mu = \mu_0(1 - R \cdot \Phi)^{-n} \quad (12)$$

where μ is the viscosity of the suspension, μ_0 is the vis-

cosity of the liquid, R is a parameter related to the critical melt fraction as $(R - 1)/R$, Φ is the volume fraction of suspended particles, and n is a constant. For the case of uniform spheres, $R = 1.35$ and $n = 2.5$. The model predicts that as $R \cdot \Phi \rightarrow 1$, the effective viscosity approaches ∞, but in reality the critical melt fraction is reached and solid-state flow laws take over. Values of $R = 1$ (critical melt fraction = 0) are reported in at least one engineering study of slurries (Lewis et al., 1949) and in one recent experimental study of a picritic composition (Ryerson et al., 1988). The data of Ryerson et al. (1988) were obtained at shear rates of ~ 1/s that are probably too high for an intruding diapir (e.g., Miller et al., 1988 calculated a shear rate of 10^{-8}/s for a granitic diapir) but nonetheless illustrate the point that the rheologies of static and moving suspensions may be quite different. Different shear rates may be part of the explanation for the absence of basaltic lavas with >55% phenocrysts among Aleutian volcanics and the presence of some picritic sills containing as much as 70% phenocrysts (Komar, 1976). For example, Marsh (1981) suggested the critical melt fraction lies at 45%.

In any case, these rheological considerations are marginally permissive of liquid-state transport of leuconoritic (leucogabbroic and leucotroctolitic) magmas with ~65% entrained plagioclase at low to moderate shear rates. It is even possible that a buoyant crystalline mush beginning to move as a granular mass would encounter a transition to liquid rheology as granulation of the crystals produced a nonuniform size distribution, thereby reducing the contiguity. The presence of a wide range of plagioclase crystal sizes from megacrysts down to millimeter-sized grains in massif anorthosite complexes is certainly consistent with such a process. Also, the mobility of a suspension would be enhanced at depth because the viscosity of the entraining silicate liquid decreases with pressure (Kushiro et al., 1976). For example, according to the empirical formulation of Perchuk (1991), liquid viscosity at lower crustal pressures (~10 kbar) would be about one-third its value at the surface.

Transport of an anorthositic mush (85% plagioclase) remains more problematic since unreasonably high shear rates are probably necessary to produce a liquid-state rheology. Not only does transport of a rheological solid through 20–25 km of continental crust seem improbable, but the high crystallinity poses thermal problems as well. Following Marsh (1982), Miller et al. (1988) pointed out that geologically reasonable ascent velocities of an igneous diapir require that the diapir continuously melts a thin layer of bounding country rock. To do this, it must convect internally to supply heat to the margins and maintain homogeneity. Thus, even though an anorthositic diapir might be 400–500 °C hotter than its surroundings (the liquidus of HLCA at 11.5 kbar is 1275 °C), its high viscosity and small latent heat content would tend to inhibit movement. Yet diapiric masses of anorthosite are observed (Wiebe, 1992).

These apparent contradictions may be alleviated by evaluating the general polybaric model in light of field studies. Working in the Laramie Complex of Wyoming, Scoates (1992) has shown that, although leucogabbroic rocks commonly contain plagioclase megacrysts, they also are commonly layered and show little or no deformation, similar to leucocratic rocks in layered intrusions, whereas in masses of more anorthositic rocks there is clear evidence of increasing deformation with increasing modal plagioclase. Mapping has shown that the major anorthositic masses lie at the core of a domal uplift, stratigraphically below the leucocratic layered rocks. Scoates (1992) has suggested that the layered rocks formed on the floor of a magma chamber with the rheological characteristics of a liquid, while the anorthosites may have formed within the cumulate pile, as the filter pressing of intercumulus liquid left buoyant, plagioclase-rich residua that became mobile, self-deforming masses. A related but different scenario may be appropriate for the relatively undeformed Michikamau Complex of Labrador. Here anorthosites overlay layered leucotroctolites and leuconorites (Emslie, 1970), and, possibly, plagioclase may have separated from the intrusive suspension within the magma chamber, rather than within the cumulate pile. Thus it may not be necessary to posit diapirs of true anorthosite intruding from the lower crust to form massif anorthosites, but rather magmatic diapirs with leuconoritic, leucotroctolitic, or leucogabbroic composition, ~65% suspended plagioclase, and liquid state rheology. Following intrusion of the leuconoritic diapirs into the upper crust and the development of magma chambers, the large masses of true anorthosites form as second-stage segregations, either as the residua of filter pressing within the cumulate pile or by floatation near the top of the chamber. These masses move only a short distance, but because of their highly crystalline nature, the movement is as a rheological solid, and thus the plagioclase within the anorthositic masses deforms and is granulated.

Acknowledgments

We wish to thank J.-C. Duchesne and R.A. Wiebe for providing rock powders used in this study. D.R. Baker, R.J. Kinzler, T. Plank, D. Walker, and R.A. Wiebe provided helpful reviews. M.S.F. was supported by an NSF graduate fellowship and NSF grant EAR-89-03410 (C.E. Lesher, P.I.). J.V.A. was supported by a Fulbright fellowship, by an FNRS grant, and by the Université de Liège. J.N.M. was an NSF summer intern at Lamont-Doherty, supported by NSF grant EAR-88-15975 (D. Walker, P.I.). Support for J.L. and most of the research was provided by NASA grant NAG-9-329. This work was also done as part of the International Geological Correlation Programme, Project 290. Lamont-Doherty Geological Observatory contribution no. 5012.

References cited

Anderson, A.T., and Morin, M. (1968) Two types of massif anorthosites and their implications regarding the thermal history of the crust. In Y.W. Isachsen, Ed., Origin of anorthosite and related rocks, p. 57–69, Memoir 18, New York State Museum and Science Service, Albany, New York.

Ariskin, A.A., and Barmina, G.S. (1990) Equilibria thermometry between plagioclases and basalt or andesite magma. Geochemistry International, 27, 129–134.

Ashwal, L.D., and Wooden, J.L. (1984) Isotopic evidence from the east-

ern Canadian shield for geochemical discontinuity in the Proterozoic mantle. Nature, 306, 679–680.

Baker, D.R., and Eggler, D.H. (1987) Compositions of anhydrous and hydrous melts coexisting with plagioclase, augite, and olivine or low-Ca pyroxene from 1 atm to 8 kbar: Application to the Aleutian volcanic center of Atka. American Mineralogist, 72, 12–28.

Barker, F., Wones, D.R., Sharp, W.N., and Desborough, G.A. (1975) The Pikes Peak Batholith, Colorado Front Range, and a model for the origin of the gabbro-anorthosite-syenite-potassic granite suite. Precambrian Research, 2, 97–160.

Bartels, K.S., Kinzler, R.J., and Grove, T.L. (1991) High pressure phase relations of a near primary high alumina basalt from Medicine Lake Highland, N. California. Contributions to Mineralogy and Petrology, 108, 253–270.

Beattie, P.D., Drake, M.J., Jones, J.H., Leeman, W.P., Longhi, J., McKay, G.A., Nielsen, R.H., Palme, H., Shaw, D.M., Takahashi, E., and Watson, E.B. (1993) A terminology for trace element partitioning. Geochimica et Cosmochimica Acta, 57, 1605–1606.

Bender, J.F., Hodges, F.N., and Bence, A.E. (1978) Petrogenesis of basalts from the Project Famous area: Experimental study from 0 to 15 kbars. Earth and Planetary Science Letters, 41, 277–302.

Berg, J.H. (1977) Dry granulite mineral assemblages in the contact aureoles of the Nain Complex, Labrador. Contributions to Mineralogy and Petrology, 64, 32–52.

Bottinga, Y., and Weill, D.F. (1972) The viscosity of magmatic silicate liquids: A model for calculation. American Journal of Science, 272, 438–475.

Boudreau, A.E. (1988) Investigations of the Stillwater Complex. IV. The role of volatiles in the petrogenesis of the J-M reef, Minneapolis adit section. Canadian Mineralogist, 26, 193–208.

Drake, M.J. (1976) Plagioclase-melt equilibria. Geochimica et Cosmochimica Acta, 40, 457–465.

Draper, N.R., and Smith, H. (1966) Applied regression analysis, 407 p. Wiley, New York.

Duchesne, J.C. (1984) Massif anorthosites: Another partisan review. In W.L. Brown, Ed., Feldspars and feldspathoids, p. 411–433. Reidel, Boston, Massachusetts.

Duchesne, J.C., and Hertogen, J. (1988) Le magma parental du lopolithe de Bjerkreim-Sokndal (Norvège méridionale). Comptes Rendus de l'Académie des Sciences (Paris), 306, 45–48.

Duchesne, J.C., and Maquil, R. (1992) The Egersund-Ogna massif. In J.C. Duchesne, Ed., The Rogaland intrusive massifs: An excursion guide, p. 7–25. International Geological Correlation Programme Project 290, Liège, Belgium.

Dymek, R.F., and Gromet, L.P. (1984) Nature and origin of orthopyroxene megacrysts from the St. Urbain anorthosite massif, Quebec. Canadian Mineralogist, 22, 297–326.

Emslie, R.F. (1970) The geology of the Michikamau intrusion, Labrador. Geological Survey of Canada Paper, 68-57, 85 p.

——— (1975) Pyroxene megacrysts from anorthositic rocks: A new clue to the sources and evolution of the parent magmas. Canadian Mineralogist, 13, 138–145.

——— (1980) Geology and petrology of the Harp Lake Complex, central Labrador: An example of Elsonian magmatism. Geological Survey of Canada Bulletin, 293, 1–136.

——— (1985) Proterozoic anorthosite massifs. In A.C. Tobi and J.L.R. Touret, Eds., The deep Proterozoic crust in the north Atlantic provinces, p. 39–60. Reidel, Dordrecht, The Netherlands.

Fram, M.S., and Longhi, J. (1992) Phase equilibria of dikes associated with Proterozoic anorthosite complexes. American Mineralogist, 77, 605–616.

Fuhrman, M., Frost, B.R., and Lindsley, D.H. (1988) Crystallization conditions of the Sybille monzosyenite, Laramie Anorthosite Complex, Wyoming. Journal of Petrology, 29, 699–729.

German, R.M. (1985) The contiguity of liquid phase sintered microstructures. Metallurgical Transactions, 16A, 1247–1252.

Green, D.H., Hibberson, W.O., and Jaques, A.L. (1979) Petrogenesis of mid-ocean ridge basalts. In M.W. McElhinny, Ed., The Earth: Its origin, structure, and composition, p. 265–299. Academic, London.

Green, T.H. (1969) High-pressure experimental studies on the origin of anorthosites. Canadian Journal of Earth Sciences, 6, 427–440.

Grove, T.L., and Bence, T.E. (1977) Experimental study of pyroxene-liquid interaction in quartz-normative basalt 15597. Proceedings of the Lunar Planetary Science Conference, 8, 1549–1579.

Grove, T.L., and Bryan, W.B. (1983) Fractionation of pyroxene-phyric MORB at low pressure: An experimental study. Contributions to Mineralogy and Petrology, 84, 293–309.

Grove, T.L., and Juster, T.C. (1989) Experimental investigations of low-Ca pyroxene stability and olivine-pyroxene-liquid equilibria at 1-atm in natural basaltic and andesitic liquids. Contributions to Mineralogy and Petrology, 103, 287–305.

Grove, T.L., Gerlach, D.C., and Sando, T.W. (1982) Origin of calc-alkaline series lavas at Medicine Lake volcano by fractionation, assimilation and mixing. Contributions to Mineralogy and Petrology, 80, 160–182.

Grove, T.L., Kinzler, R.J., and Bryan, W.B. (1992) Fractionation of mid-ocean ridge basalt. In J. Phipps-Morgan, D.K. Blackman, and J.M. Sinton, Eds., Mantle flow and melt migration at mid-ocean ridges: Geophysical Monograph 71. American Geophysical Union, Washington, DC.

Hess, P.C. (1980) Polymerization model for silicate melts. In R.B. Hargraves, Ed., Physics of magmatic processes, p. 1–48. Princeton University Press, Princeton, New Jersey.

Holloway, J.R., Pan, V., and Gudmundsson, G. (1992) Melting experiments in the presence of graphite: Oxygen fugacity, ferrous/ferric ratio and dissolved CO_2. European Journal of Mineralogy, 4, 105–114.

Housh, T.B., and Luhr, J.F. (1991) Plagioclase-melt equilibria in hydrous systems. American Mineralogist, 76, 477–492.

Jurewicz, S.R., and Watson, E.B. (1985) The distribution of partial melt in a granitic system: The application of liquid phase sintering theory. Geochimica et Cosmochimica Acta, 49, 1109–1122.

Kinzler, R.J., and Grove, T.L. (1992) Primary magmas of mid-ocean ridge basalts. I. Experiments and methods. Journal of Geophysical Research, 97, 6885–6906.

Kirkpatrick, R.J. (1977) Nucleation and growth of plagioclase, Makaopuhi and Alae lava lakes, Kilauea Volcano, Hawaii. Geological Society of America Bulletin, 88, 78–84.

Komar, P.D. (1976) Phenocryst interactions and the velocity profile of a magma flowing through dikes or sills. Geological Society of America Bulletin, 87, 1336–1342.

Kushiro, I., Yoder, H.S., Jr., and Mysen, B.O. (1976) Viscosity of basalt and andesite melts at high pressure. Journal of Geophysical Research, 81, 6351–6359.

Lesher, C.E. (1991) Chemical and self diffusivities of Sr and Nd in naturally-occurring silicate liquids (abs.). Eos, 72, 309.

Lewis, W.K., Gilliland, E.R., and Bauer, W.C. (1949) Characteristics of fluidized particles. Industrial Engineering and Chemistry, 41, 1104–1117.

Longhi, J., and Ashwal, L.D. (1984) A two stage model for lunar anorthosites: An alternative to the magma ocean hypothesis. Journal of Geophysical Research, 90, C571–C584.

Longhi, J., and Pan, V. (1988) A reconnaissance study of phase boundaries in low-alkali basaltic liquids. Journal of Petrology, 29, 115–148.

——— (1989) The parent magmas of the SNC meteorites. Proceedings of the Lunar Planetary Science Conference, 19, 451–464.

Mahood, G.A., and Baker, D.R. (1986) Experimental constraints on depths of fractionation of mildly alkalic basalts and associated felsic rocks: Pantelleria, Strait of Sicily. Contributions to Mineralogy and Petrology, 93, 251–264.

Maquil, R. (1978) Preliminary investigation on giant orthopyroxenes with plagioclase exsolution lamellae from the Egersund-Ogna anorthositic massif (S. W. Norway). National Energy Research Council Publication Series D, 4, 144–146.

Marsh, B.D. (1981) On the crystallinity, probability of occurrence and rheology of lava and magma. Contributions to Mineralogy and Petrology, 78, 85–98.

——— (1982) On the mechanics of igneous diapirism, stoping, and zone melting. American Journal of Science, 282, 808–855.

Meen, J.K. (1990) Elevation of potassium content of basaltic magma by fractional crystallization: The effect of pressure. Contributions to Mineralogy and Petrology, 104, 303–331.

Miller, C.F., Watson, E.B., and Harrison, M.T. (1988) Perspectives on

the source, segregation and transport of granitoid magmas. Transactions of the Royal Society of Edinburgh: Earth Sciences, 79, 135–156.

Morse, S.A. (1975) Plagioclase lamellae in hypersthene, Tikkoatokhakh Bay, Labrador. Earth and Planetary Science Letters, 26, 331–336.

——— (1982) A partisan review of Proterozoic anorthosites. American Mineralogist, 67, 1087–1100.

Morse, S.A., and Nolan, K.M. (1984) Origin of strongly reversed rims on plagioclase in cumulates. Earth and Planetary Science Letters, 68, 485–498.

Nicholson, D.M., and Mathez, E.A. (1991) Petrogenesis of the Merensky Reef in the Rustenburg section of the Bushveld Complex. Contributions to Mineralogy and Petrology, 107, 293–309.

Nielsen, R.L., and Dungan, M.A. (1983) Low pressure mineral-melt equilibria in natural anhydrous mafic systems. Contributions to Mineralogy and Petrology, 84, 310–326.

Pan, V., and Longhi, J. (1990) The system Mg_2SiO_4-Ca_2SiO_4-$CaAl_2O_4$-$NaAlSiO_4$-SiO_2: One atmosphere liquidus equilibria analogs of alkaline magmas. Contributions to Mineralogy and Petrology, 105, 569–584.

Perchuk, L.L. (1991) The viscosity of magmatic silicate liquids: Experiment, generalized patterns. A model for calculation and prediction. Applications. In L.L. Perchuk and I. Kushiro, Eds., Physical chemistry of magmas, p. 1–40. Springer-Verlag, New York.

Ryerson, F.J., Weed, H.C., and Piwinskii, A.J. (1988) Rheology of subliquidus magmas. I. Picritic compositions. Journal of Geophysical Research, 93, 3421–3436.

Scoates, J.S. (1992) Anorthosites in the Laramie Anorthosite Complex, Wyoming, USA: Structural and geochemical evidence for a complex emplacement, crystallization, and deformational history (abs.). In J.C. Duchesne, Ed., Magma chambers and processes in anorthosite formation, p. 21. International Geological Correlation Programme Project 290, Liège, Belgium.

Scoates, J.S., and Lindsley, D.H. (1989) Primary layering and structures within a ca. 1.43 Ga massif anorthosite, Laramie Anorthosite Complex, S. E. Wyoming. Geological Association of Canada–Mineralogical Association of Canada Program with Abstracts, 14, A5.

Sen, G., and Presnall, D.C. (1984) Liquidus phase relations on the join anorthite-forsterite-quartz at 10 kbar with applications to basalt petrogenesis. Contributions to Mineralogy and Petrology, 85, 404–408.

Shaw, H.R. (1965) Comments on viscosity, crystal settling, and convection in granitic magmas. American Journal of Science, 263, 120–152.

Smith, V.G., Tiller, W.A., and Rutter, J.W. (1955) A mathematical analysis of solute redistribution during solidification. Canadian Journal of Physics, 33, 723–745.

Stolper, E.M. (1980) A phase diagram for mid-ocean ridge basalts: Preliminary results and implications for petrogenesis. Contributions to Mineralogy and Petrology, 74, 13–27.

Streckeisen, A.L. (1976) To each plutonic rock its proper name. Earth Science Reviews, 12, 1–34.

Thy, P. (1991) High and low pressure phase equilibria of a mildly alkalic lava from the 1965 Surstsey eruption: Experimental results. Lithos, 26, 223–243.

Valley, J.W., and O'Neill, J.R. (1978) Oxygen isotope evidence for shallow emplacement of Adirondack anorthosite. Nature, 300, 497–500.

Vander Auwera, J., and Longhi, J. (1992) Phase equilibria and fractionation paths from 1 atm up to 16 kb of the monzonoritic Tjorn chilled facies: Implications for the Bjerkreim-Sokndal Lopolith (southern Norway) (abs.). In J.C. Duchesne, Ed., Magma chambers and processes in anorthosite formation, p. 25. International Geological Correlation Programme Project 290, Liège, Belgium.

van der Molen, I., and Paterson, M.S. (1979) Experimental deformation of partially molten granite. Contributions to Mineralogy and Petrology, 70, 299–318.

Waff, H.S., and Faul, U.F. (1992) Effects of crystalline anisotropy on fluid distribution in ultramafic partial melts. Journal of Geophysical Research, 97, 9003–9014.

Weaver, J.S., and Langmuir, C.H. (1990) Calculation of phase equilibrium in mineral-melt systems. Computers and Geosciences, 16, 1–19.

Wiebe, R.A. (1979) Anorthositic dikes, southern Nain Complex, Labrador. American Journal of Science, 279, 394–410.

——— (1986) Lower crustal cumulate nodules in Proterozoic dikes of the Nain Complex: Evidence for the origin of Proterozoic anorthosites. Journal of Petrology, 27, 1253–1275.

——— (1990) Evidence for unusually feldspathic liquids in the Nain Complex, Labrador. American Mineralogist, 75, 1–12.

——— (1992) Proterozoic anorthosite complexes. In K.C. Condie, Ed., Proterozoic crustal evolution, p. 215–261. Elsevier, Amsterdam.

Manuscript received October 8, 1992
Manuscript accepted May 25, 1993